New three dimensional models of interstellar gas and their impact on high-energy interstellar emission.

Guðlaugur Jóhannesson[1], Igor V. Moskalenko[2], and Troy A. Porter[2]

[1]Science Institute, University of Iceland, Dunhaga 3, IS-105 Reykjavík, Iceland

[2]W.W. Hansen Experimental Physics Laboratory, Stanford University, Stanford, CA 94305, USA

Three dimensional ISM models

The Milky Way is a barred spiral arm Galaxy with a large fraction of its interstellar medium and star formation activities contained in the spiral arms. Despite this most models of cosmic-rays (CRs) in the Milky Way have used 2D azimuthally symmetric distributions. We have developed a method to determine the 3D distribution of interstellar gas that is suitable for input into CR propagation codes. The resulting distributions are shown in figure 1. Using the GALPROP propagation code we study how including these distributions affect the resulting high-energy γ-ray emission when combined with a CR source distribution with spiral arms that results in the CR energy density shown in figure 2. Using the new gas models results in slower CR diffusion that enhances the effect of moving to a 3D CR source distribution. The effect on the interstellar emission is shown in figures 3 and 4
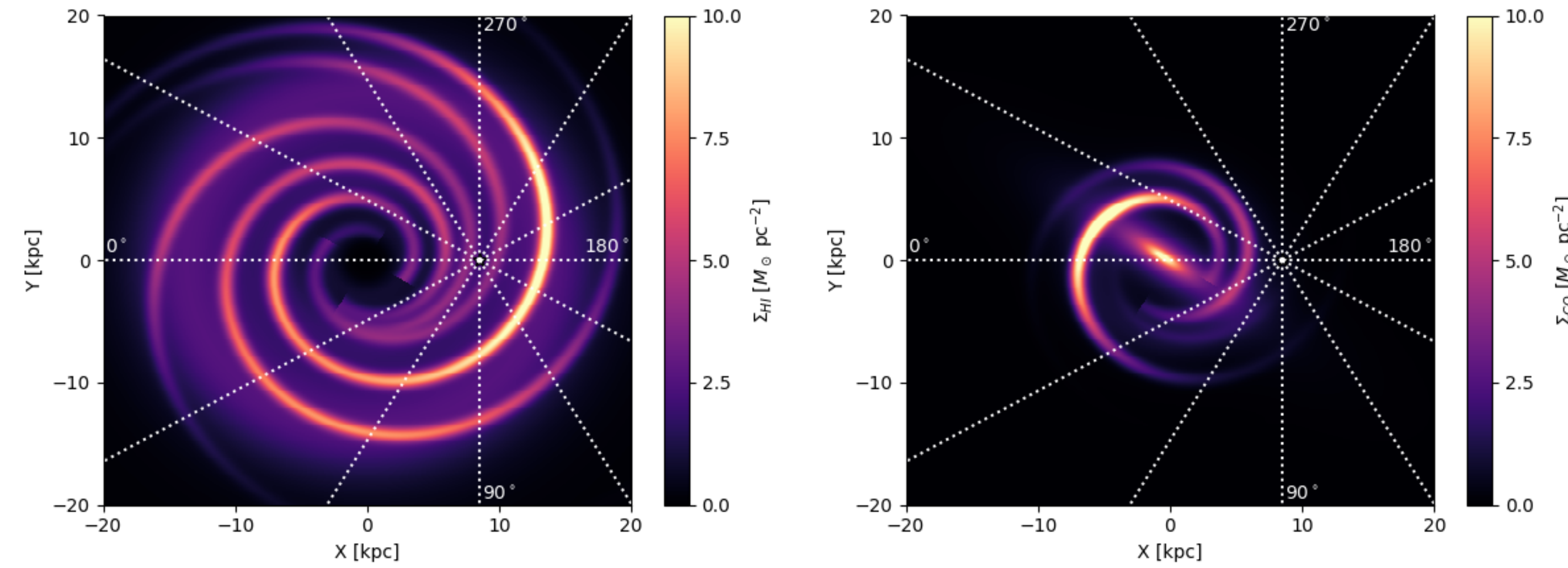
3D gas distributions

Figure 1: *Top down view of the Milky Way showing the surface density of the H I and H$_2$ gas using our new models for the 3D distribution of interstellar gas. The enhanced gas densities along the spiral arm structures are apparent.*
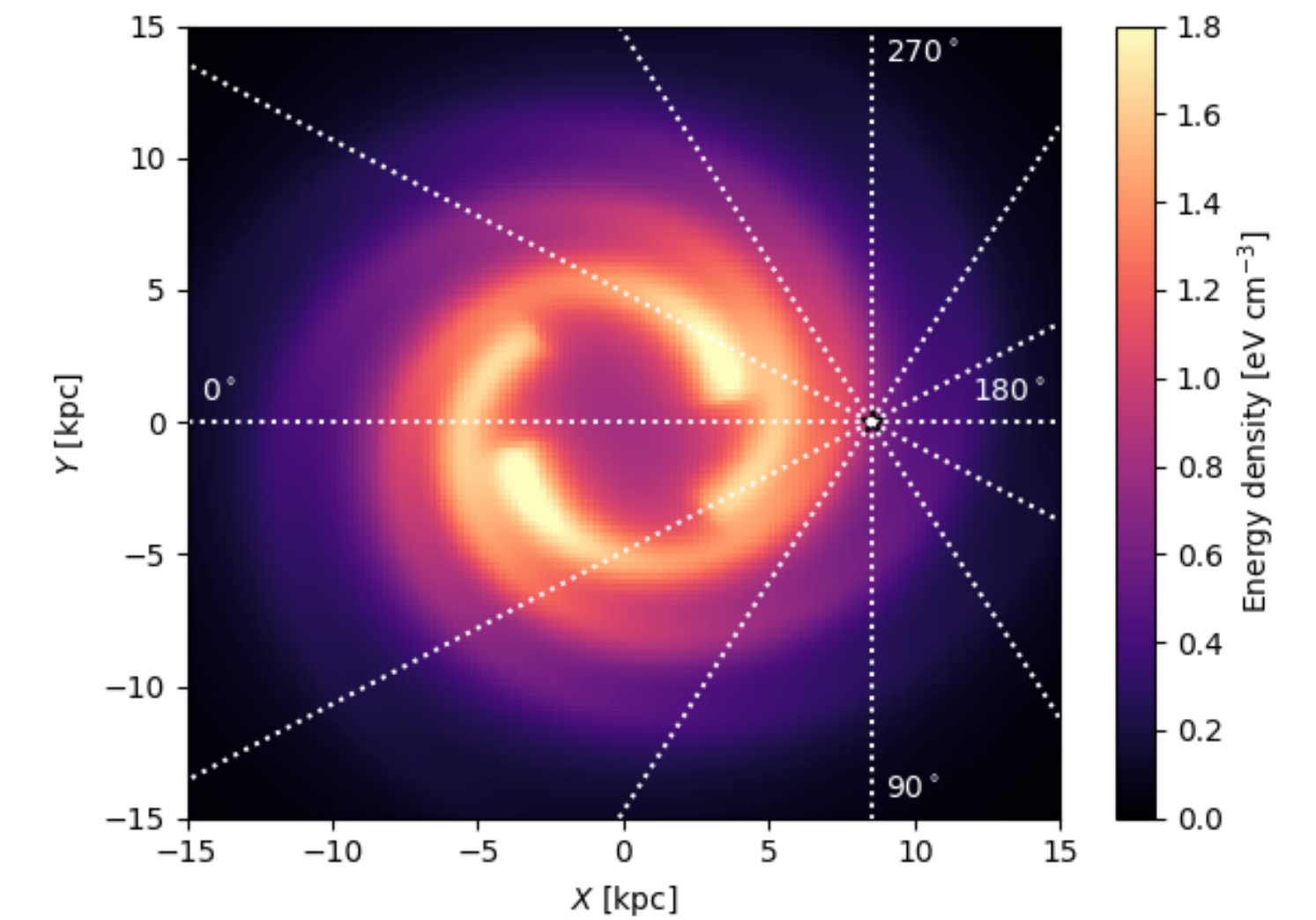
3D CR distribution

Figure 2: *The CR energy density of our model after propagation.*
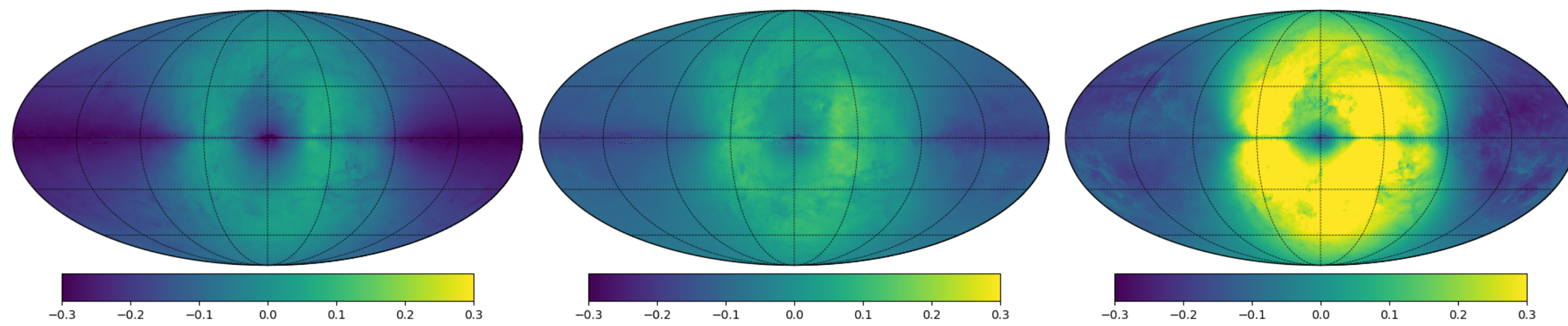
Interstellar emission with 3D CRs

Figure 3: *Ratio of the total γ-ray intensity of models incorporating 3D structure in the CRs compared to a model with 2D symmetric models for both gas and CRs. Shown are maps for the ratio at 30 MeV, 1 GeV, and 100 GeV from left to right. The intensity maps have been calculated with GALPROP. The enhanced intensity due to the CR spiral arm features are visible as a doughnut like excess.*
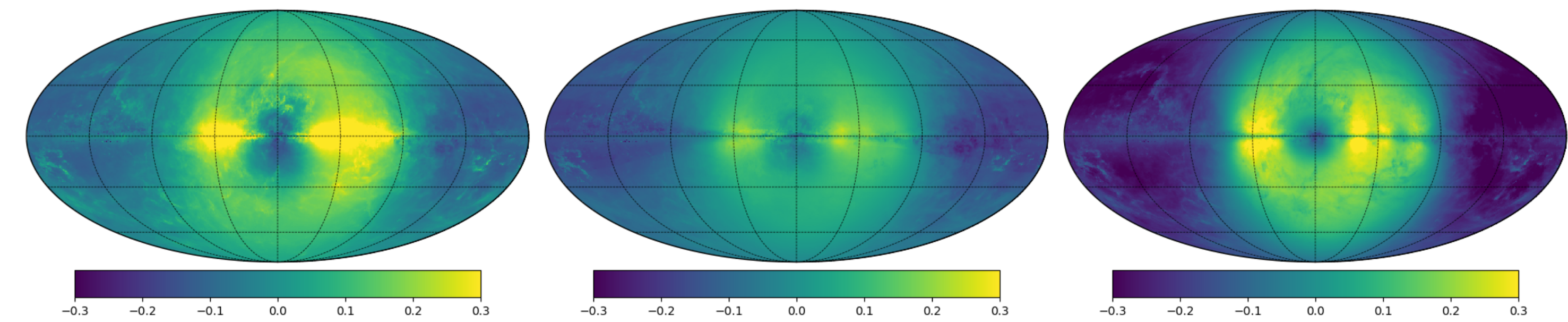
Interstellar emission with 3D CRs and gas

Figure 4: *Ratio of the total γ-ray intensity of a model using 3D structure in both CRs and interstellar gas compared to a model with 2D symmetric models for both gas and CRs. Shown are maps for the ratio at 30 MeV, 1 GeV, and 100 GeV from left to right. The intensity maps have been calculated with GALPROP. Compared to the maps in figure 3 the enhanced intensity due to the CR spiral arm features are more confined to the plane and individual spiral arms can be seen at the highest energies.*

1 Introduction

The interstellar emission resulting from cosmic rays (CRs) interacting with the interstellar medium (ISM) in the Galaxy is a prominent feature of the γ-ray sky and is responsible for more than half of the photons observed by the *Fermi*–LAT. Most of the current interstellar emission models (IEMs) assume a 2D cylindrically symmetric distribution of CRs [1, 2]. While they provide a reasonable fit to the *Fermi*–LAT data, residuals of the order of few tens of percent are visible on scales ranging from a few to tens of degrees. Some of those are likely related to large scale structures in the CR and ISM that is not encapsulated in the 2D models. These new data have inspired progress towards a more detailed 3D models for the high energy interstellar emission [3, 4, 5]. This work follows a similar path focusing on the distribution of interstellar gas and how its distribution affects the expected distribution of CRs.

Knowledge of the distribution of interstellar gas comes mostly from observation of the H I 21-cm line and CO 2.6-mm line [6]. The line emission strength is related to the column density of interstellar gas and under assumptions of cylindrical gas motion the Doppler shift of the emission lines can be used to infer the distance to the emitting gas. This gives a direct mapping from the observed line emission (l, b, v) to the density of interstellar gas (x, y, z) [7, 8, 9]. This mapping is however not without issues. Thermal and turbulent motions of the gas create a spread in the Doppler shift that directly relates back to spread in distance estimates resulting in elongated features along lines of sight. The gas is also not in a purely cylindrical motion around the Galactic centre (GC) and those non-cylindrical velocities dominate the Doppler shift along directions towards and away from the GC resulting in regions with no distance information. In this work we instead use the inverse mapping $(x, y, z) \rightarrow (l, b, v)$ and parameterise the gas density distribution. The parameters are adjusted in a maximum likelihood fit to the emission line data. This enforces continuity across directions were non-cylindrical motions dominate and reduces the effect of random gas motion because smoothing is applied to the model. This comes at the expense of fine structure in the model that is difficult to account for unless the number of parameters in the model becomes unreasonably large.

2 3D modeling of the interstellar gas

The parameters of the model are optimised using a maximum-likelihood fit to the H I LAB survey [10] and the DHT CO survey [11]. The survey data is re-binned to a HEALPix grid [12] using HEALPix order 7 for H I while order 8 is used for the CO data. The spatial resolution is chosen to resolve the latitudinal dependence of the gas distribution toward the GC. The velocity resolution of both surveys is degraded to 2 km s^{-1}, which is smaller than the expected line broadening due to turbulent and thermal emotion that is assumed to be 6 km/s and 10 km/s for CO and H I respectively. The statistical uncertainty on the data is assumed to be constant over the entire sky and values of 0.05 K for CO and 0.1 K for HI are assumed, which are in agreement with the noise estimate for the original surveys taking into account the re-binning. Even though the noise in the surveys is normally distributed, a student-t likelihood is used to reduce sensitivities to large outliers that are inevitable because the model cannot capture the finest structures in the line emission observations.

The model consists of two parts, the density of the gas $n_x(\vec{X})$ and the velocity field of the gas $\vec{v}(\vec{X})$, where $\vec{X}$ is the position in the Galaxy and the subscript x can be either H I or CO. For each line-of-sight the velocity field is used to calculate the expected Doppler shift as a function of distance to set the integration boundaries of the model. The density is then integrated along the line-of-sight and converted to line intensity. For H I the radiative transport equation is used to estimate the line intensity assuming the gas is optically thin. For CO the line intensity is assumed linearly related to the density, which is suitable if the final model is turned into H$_2$ densities using the X_{CO} factor.

For this contribution we use a simple geometrical models for the density and cylindrical rotation using the rotation curve from [13]. Because the model does not provide any distance information around the GC and anti-centre the velocity information within $\pm 10°$ longitude about both centres is ignored and only the velocity integrated emission is used to form the likelihood. The models are built iteratively, starting with a 2D disc model and then adding more complex features as necessary. The added features comprise: warping of the disc, a central bulge/bar, flaring in the outer Galaxy, and spiral arms. The warp and the flaring are significant only in the outer Galaxy and therefore do not have a large effect on the CO analysis that has only a small amount of gas in the outer Galaxy. The
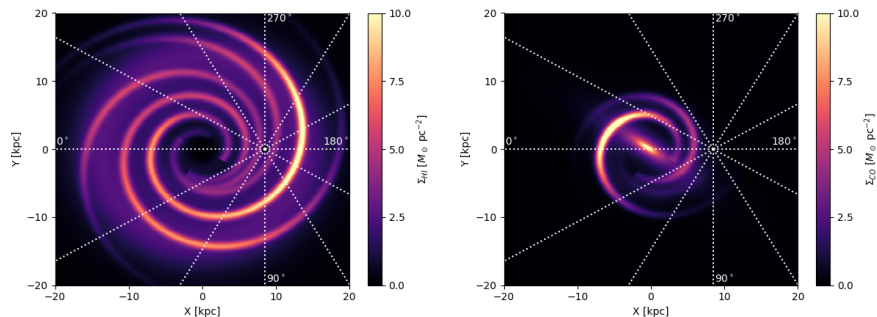
Figure 1: Surface density maps of the final models with H I on left and CO on right. The CO model is converted to surface density assuming $X_{CO} = 2 \cdot 10^{20}$ cm^{-2} K^{-1} (km/s)$^{-1}$. The sun is marked as a white point and the dashed lines show directions of longitudes at 30° intervals.
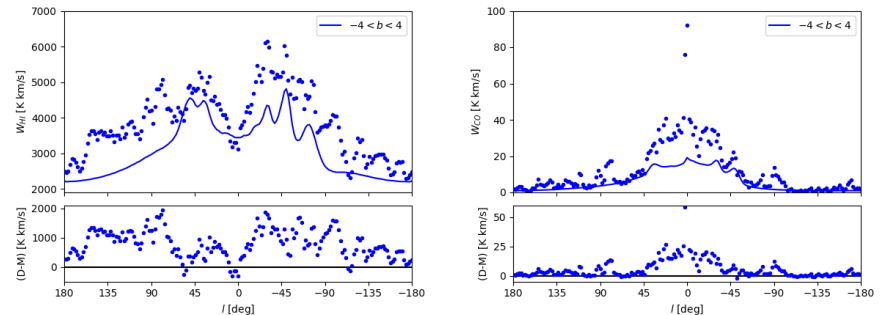

Figure 2: Longitude profile of the models (curves) overlaid on the data (points). The model and data are integrated over all velocity bins and averaged over the latitude range $-4° < b < 4°$. H I is on left and CO on right.

bulge/bar has only a small effect for the H I and the density ascribed to this component from the analysis is insignificant. Adding logarithmic spiral arms gives a significant improvement for both atomic and molecular gas models.

The surface density of the final distribution is shown in figure 1. The spiral arms are prominent in both H I and CO and the central bulge in CO. The model parameters were set such that the shape of the spiral arms are identical in both models, the radial density distribution is identical for the disk and spiral arms in each model but the relative contribution of each arm is free. For CO the density of one of the arms is effectively put to 0 and another is a factor ~ 10 less dense than the densest arm and therefore barely visible in the figure. Comparison of the models to data is shown in the velocity integrated longitude profiles along the plane in figure 2. The model systematically under predicts the data which is to be expected when using the student-t likelihood that de-weights the tail of the residual distribution that is in this case dominated by positive residuals. This was by design so missing components would more easily show up as positive structures in the residuals. The spiral arm features are clearly visible in the model profiles as peaks and they match similar features in the data. The model chosen for this work is clearly not capable of reproducing all the complex features of the data even though the spiral arm structure reasonably matches that of the data.

3 Interstellar emission models

To demonstrate the effects these new gas distributions have on IEMs we incorporate them into the $GALPROP$ code [14, 4]. The gas distributions in $GALPROP$ are used for the calculation of energy losses and the production of secondary particles while the final γ-ray intensity maps are scaled such that the column density of each line of sight matches that estimated from the line surveys. The change in gas distributions therefore only affects the CR part of the IEM, the gas column density is corrected to match the observations. For simplification we only consider here a diffusive re-acceleration model with a homogeneous and isotropic diffusion with the CR sources distributed concentrated in spiral arms using the SA100 model from [4]. The CR source distribution is combined with the old 2D gas distributions from $GALPROP$ and the new 3D gas distributions resulting in two new models. These models are compared to a model having the 2D CR source distribution SA0 and the old 2D gas distribution.

The CR propagation parameters are tuned to match observations of secondary CRs whose predictions depends on both the gas and CR source distribution. To have a consistent comparison, the propagation parameters of each of the 3 models is tuned to the same CR data. The new gas distributions have a large effect on the propagation parameters, reducing

the diffusion coefficient and the Alfvén speed by a factor of ~ 2. This is because the integrated column density of the new distributions around the location of the sun is smaller by about a factor of 2 resulting in less production of secondaries that is compensated for by having slower diffusion. The energy losses of the CRs are also affected and the estimated parameters for solar modulation and low energy CR injection are affected by the change in gas distribution.

The effect on the interstellar emission is illustrated in figure 3 that shows the ratio of the total γ-ray intensity of the models employing the SA100 CR source distribution to the reference model with the SA0 distribution. The 3D CR source distribution results in a doughnut like excess centred on the GC that is caused by a general increase in CR flux in the inner Galaxy combined with lack of CR sources near the GC. The reduced diffusion in the model with the new gas distribution results in a more confined excess around the plane and less emission in the outer Galaxy. The increased emission at low energies is a result of the change in modulation during the tuning of the propagation parameters.

References

[1] Ackermann, M., et al. 2012, ApJ, 750, 3

[2] Ajello, M., et al. 2016, ApJ, 819, 44

[3] Johannesson, G., Moskalenko, I. V., & Porter, T. 2013, Br. J. of Phys., ICRC2013, 0913

[4] Porter, T. A., Johannesson, G., & Moskalenko, I. V. 2017, ArXiv e-prints

[5] Kissmann, R., Niederwanger, F., Reimer, O., & Strong, A. W. 2017, in American Institute of Physics Conference Series, Vol. 1792, 6th International Symposium on High Energy Gamma-Ray Astronomy, 070011

[6] Ferrière, K. M. 2001, Reviews of Modern Physics, 73, 1031

[7] Levine, E. S., Blitz, L., & Heiles, C. 2006, ApJ, 643, 881

[8] Pohl, M., Englmaier, P., & Bissantz, N. 2008, ApJ, 677, 283

[9] Nakanishi, H., & Sofue, Y. 2016, PASJ, 68, 5

[10] Kalberla, P. M. W., et al. 2005, A&A, 440, 775

[11] Dame, T. M., Hartmann, D., & Thaddeus, P. 2001, ApJ, 547, 792

[12] Górski, K. M., et al. 2005, ApJ, 622, 759

[13] Sofue, Y., Honma, M., & Omodaka, T. 2009, PASJ, 61, 227

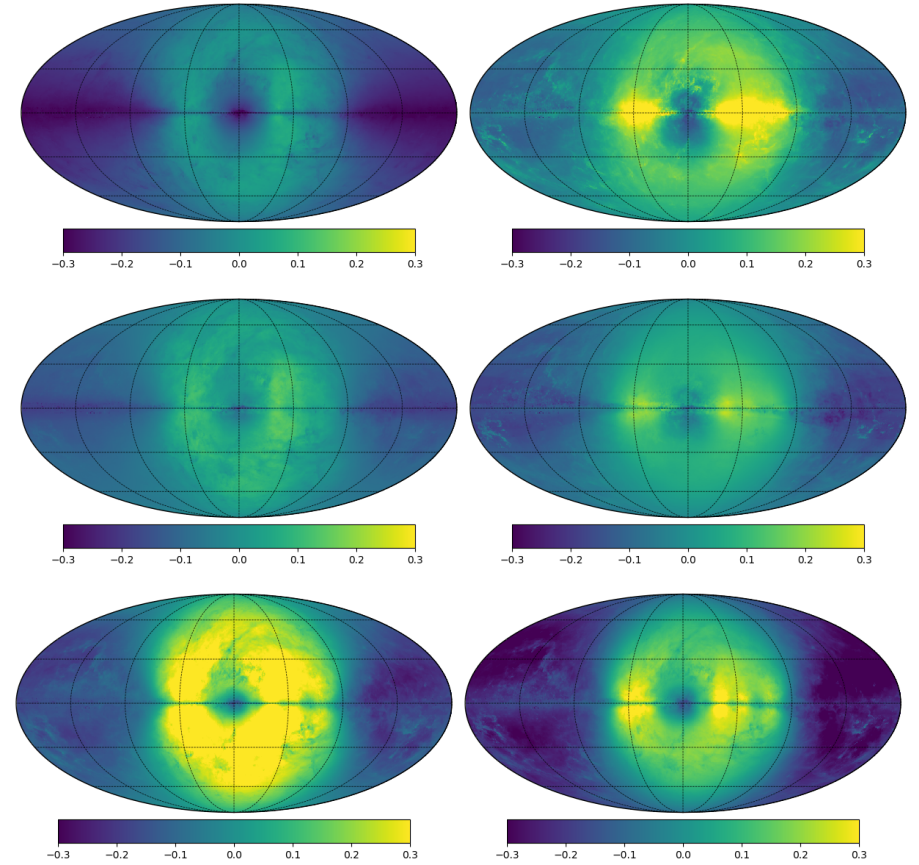[14] Vladimirov, A. E., et al. 2011, Computer Physics Communications, 182, 1156

Figure 3: Fractional residuals for the total γ-ray intensity (π^0-decay, Bremsstrahlung, and IC) at 30 MeV, 1.0 GeV, and 100 GeV energies (top to bottom, respectively) for SA100-2D gas (left) and SA100-3D gas (right) compared to 2D CR and gas reference model. The maps are in Galactic coordinates with $l, b = 0°, 0°$ at the centre with l increasing to the left. The longitude meridians have $45°$ spacing and latitude parallels have $30°$ spacing.